Macromolecules

Volume 40, Number 7 April 3, 2007

Review

Selected Issues in Liquid Crystal Elastomers and Gels

Kenji Urayama†

Department of Materials Chemistry, Kyoto University, Kyoto 615-8510, Japan

Received October 16, 2006; Revised Manuscript Received January 24, 2007

ABSTRACT: In this perspective, we discuss select issues investigated in recent studies on liquid crystal elastomers (LCEs) and gels—soft solids having a mobile director. A considerable amount of knowledge accumulated during the past decade proves that LCEs are not simple extensions of liquid crystals (LCs) and elastomers. The strong coupling of orientational order of LCs and rubber elasticity of polymer networks leads to novel stimulus-response behavior that provides not only a wealth of academically interesting issues but also numerous potential applications including soft actuators, components of artificial muscles, and nonlinear optical devices. We mainly focus on the responses of LCEs swollen by a low molecular mass LC to the temperature variations and electric fields. The temperature response reveals that their macroscopic volume and shape are strongly coupled with nematic order; therefore, they behave as the anisotropic gels with temperature-responsive volume and shape. In fast response to electric fields, the swollen LCEs exhibit a macroscopic deformation as well as a significant change in birefringence. This pronounced electrooptical and mechanical effect suggests that they are promising materials for electrically driven soft actuator, and it also provides an important basis to understand a LCE-specific deformation mode induced during a 90° rotation of director. We also highlight some characteristic textures and distortions driven by director realignment observed in the frustrated LCEs under mechanically constrained geometries. In addition, we discuss the phase transition and slow dynamics specific to polydomain LCEs having disordered directors. We summarize the unresolved and challenging issues regarding these topics.

1. Introduction

Liquid crystal elastomers (LCEs) are unique solid materials possessing a mobile director and rubber elasticity. LCEs comprise rubbery networks of cross-linked polymer chains that have rodlike elements sufficient to induce a mesophase. LCEs are often referred to as a new class of materials owing to their hybrid characteristics—a cross between liquid crystals (LCs) and elastomeric solids. Unlike un-cross-linked LC polymers, LCEs behave as solids; i.e., they do not flow because cross-linking prohibits the motion of entire molecules. Nevertheless, the mesogenic groups in LCEs still have considerable mobility because the network backbone formed by distant adjacent cross-links is in the rubbery state. The concept of LCEs was first envisaged by de Gennes;[1] a considerable amount of knowledge in this field has been accumulated since Küpfer and Finkelmann pioneered a method of producing globally aligned monodomain LCEs in 1991.[2] It proves that LCEs exhibit several novel properties that are not simple extensions of the inherent characteristics of LCs and elastomers.[3−7] The most important characteristic of LCEs is the strong coupling of the orientational order of LCs with the rubber elasticity of polymer networks. The alignment of the constituent mesogens is always coupled with the macroscopic shape of the LCEs, and vice versa. A remarkable property arises due to this characteristic: uniaxial spontaneous deformation in response to various environmental factors (such as temperature and light irradiation) affecting their orientational order parameter. Externally imposed deformation can also realign the director along the stretching

† E-mail: urayama@rheogate.polym.kyoto-u.ac.jp.

10.1021/ma0623688 CCC: $37.00
Published on Web 03/06/2007

Kenji Urayama is currently an Associate Professor of Materials Chemistry at Kyoto University, Japan, after being an Assistant Professor in the Institute for Chemical Research at Kyoto University. He earned a Ph.D. in Materials Chemistry from Kyoto University in 1996. His research mostly focuses on fundamentals of the stimulus-response behavior in polymer gels and elastomers. His honors include the 2006 John H. Dillon Medal from the Division of Polymer Physics of the American Physical Society (2006).

direction. Importantly, LCEs exhibit a memory effect regarding their director in the preparation state, and the mesogen alignment recovers its original state when the external factors are initialized.

Various LCEs including nematic, cholesteric, smectic A, smectic C*, and discotic LCEs have been synthesized and characterized.[5,6] These LCEs have numerous potential applications such as soft actuators, artificial muscles, and nonlinear optical devices. The coupling of the mesogen alignment with elastomeric networks also yields many academically interesting issues such as nonsymmetric elasticity, unusual phase transition, and significantly nonlinear mechanical responses. These issues have been the subjects of many publications. The initial studies and recent advances in this field have been summarized in a book[5] and review articles.[3,4,6,7] The main aim of this perspective is to focus on some new topics that were not studied in these earlier reviews and to focus attention on the unresolved issues and future challenges regarding these topics. We restrict here ourselves to the investigation of nematic LCEs. In section 2, we discuss the current status and future direction of research regarding the synthetic aspects of LCEs. In section 3, we describe the response of LCEs immersed in solvents to temperature changes. Most of the earlier studies have focused on temperature-induced shape changes in the dry state without volume change.[2−7] LCEs immersed in solvents undergo variations in volume as well as shape, and they behave as the anisotropic gels having temperature-responsive volume and shape. The rubber elasticity of nematic networks leads to some interesting features in the phase diagrams that are absent in uncross-linked liquid crystal polymer/solvent and non-nematogenic network/solvent systems. In section 4, we describe pronounced electromechanical and optical effects observed in a monodomain LCE swollen by a nematic solvent without external constraints. The electric field effect with response times of ca. 10 ms and induced strains of more than 10% demonstrates that the LCEs can be promising materials for a soft actuator having high actuation speed. This electric field response also reveals an LCE-specific deformation pathway during a 90° rotation of the director. Further, we introduce some inhomogeneous textures and distortions (such as the Fréedericksz effect and buckling deformation) of frustrated LCEs in a constrained geometry.

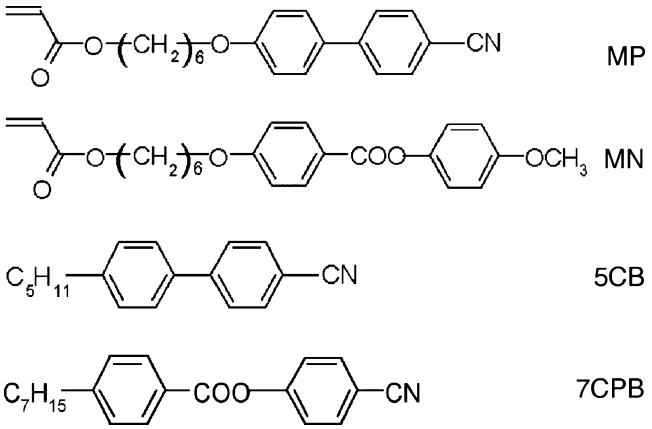

Figure 1. Chemical structures of the reactive mesogens MP and MN and low-molecular-mass LCs 5CB and 7CPB.

These inhomogeneous realignments of the director reveal the coupling of two types of elasticities originating from elastomeric networks and LCs. In section 5, we focus on disordered polydomain LCEs without a global director but with local nematic alignment of the order of microns. Polydomain LCEs have not been sufficiently studied as compared to monodomain LCEs because the disordered mosaic texture effectively masks the macroscopic anisotropy. We show a striking difference in phase transition between swollen monodomain and polydomain LCEs. Further, we introduce the slow dynamics of the shape recovery arising from the polydomain nature.

2. Classifications and Preparation Schemes

LCEs are categorized into main-chain- and side-chain-type LCEs in a manner similar to conventional LC polymers depending on whether the rodlike elements are concatenated along or pendant to the network backbone.[8] These two LCEs exhibit no qualitative difference in their physical behavior. However, the anisotropy of the backbone chains in main-chain LCEs is much greater than that in side-chain LCEs due to the direct coupling of the mesogen alignment and backbone conformation. As a result, the nematic effect on the macroscopic properties is more pronounced in main-chain LCEs than in side-chain LCEs.[9,10] Most of the previous experimental studies have employed side-chain LCEs because main-chain LCEs are usually more difficult to synthesize than side-chain LCEs. Efforts should be continued to investigate a simple synthesis route for main-chain LCEs in order to pursue high-performance LCEs.[11]

Another important classification—*monodomain or polydomain* LCEs—is based on the presence or absence of a global director. Monodomain LCEs having global alignment show a considerable anisotropy in various macroscopic properties. Such macroscopic anisotropy is absent in polydomain LCEs due to their disordered director orientation. If the mesogen alignment during the cross-linking stage is not carefully controlled, the resultant LCEs exhibit a polydomain mosaic texture without a global director. One of the familiar methods to form monodomain LCEs is the two-step cross-linking technique that was pioneered by Küpfer and Finkelmann.[2] In the first stage, the partial cross-linking yields a nematic network with a polydomain texture. The second cross-linking is performed on the first network in the uniaxially stretched state inducing a mesogen orientation, which results in a monodomain LCE. This method has been used in many studies, although it is a considerably complicated and delicate two-step process. Alternative methods employ a magnetic field,[12,13] mechanical stretching,[14] balloon inflation,[15]

or anchoring force arising from rubbed polymer layers[16,17] in order to align the mesogens upon cross-linking. Substantially, the cross-linking reaction under these aligning fields is a one-step process. For example, the author's group prepared a monodomain side-chain-type LCE based on acrylate backbone by photo-cross-linking the reactive mesogen MP or MN (Figure 1) and cross-linker 1,6-hexanediol diacrylate in the glass cell whose surfaces are coated with uniaxially rubbed polyimide layer.[17] The free-standing LCE films of a thickness of 20−100 μm with macroscopic uniaxial mesogen alignment are obtained by separating from the glass substrates.[16,17]

Several researchers have developed LC gels[18] or LCEs[19] utilizing the microphase separation of ABA triblock copolymers whose central block is an LC polymer. The global director is formed by fiber drawing,[19] surface treatment of a cell, or application of magnetic fields.[18] This method has the advantage of not requiring a cross-linking reaction. An important challenge is the development of more sophisticated and simple synthesis routes for LCEs having high nematic anisotropy, particularly from the viewpoint of practical applications.

3. Volume and Shape Coupled with Nematic Order

The spontaneous deformation of LCEs induced by temperature (T) variations has been the subject of many studies during the past decade. Temperature variations, particularly across the nematic−isotropic (NI) transition temperature (T_{NI}), readily induce large changes in the nematic order parameter of LCEs. The resultant emergence or increase in the nematic order drives a spontaneous elongation along the director, whereas its disappearance or decay induces a reverse deformation. Such T-induced deformation of LCEs has been summarized in a book.[5] This spontaneous distortion in the neat state involves no volume change. Here, we focus on the response of LCEs immersed in solvents to T changes. When an LCE is immersed in a solvent, it can change its volume by absorbing or expelling the solvent according to the balance of the chemical potentials of the solvent inside and outside the network. In this case, the nematic order is strongly coupled with volume as well as shape, and the resultant swelling becomes considerably anisotropic. This complicates the swelling of LCEs to a greater extent than that of non-nematogenic elastomers and also leads to the interesting gels having temperature-responsive volume and shape. In addition, the principal difference between the LCE/solvent and un-cross-linked LC polymer/solvent systems is that the former always has a phase gap between the swollen network and the pure surrounding solvent owing to cross-linking. In the past 5 years, the behavior of swollen LCEs has been experimentally revealed in detail. Several experimental studies have employed an LCE swollen by solvents;[20−23] however, detailed phase diagrams focusing on equilibration at each T have not been obtained because the main focus was on other physical properties.

Figure 2a shows the schematic diagram of the T dependence of equilibrium volume and shape of monodomain LCEs immersed in non-nematogenic solvents.[17] Nematic ordering occurs at T_{NI}^{G}, which is the NI transition temperature not in the dry state (T_{NI}^{N}) but in the fully swollen state, i.e., the state of a miscible mixture of LCE and solvent with a certain LCE volume fraction at T_{NI}^{G}. The temperature T_{NI}^{G} becomes considerably lower than T_{NI}^{N} owing to a dilution effect of the non-nematogenic solvent on network nematicity. The nematic ordering drives a reduction in gel volume as well as an elongation along the director. The LCEs in the high-T isotropic region swell considerably without anisotropy. In the low-T nematic region, the network shrinks and elongates along the director. In the nematic regime, the degree of equilibrium swelling is almost T-independent, whereas the shape anisotropy increases with cooling, particularly near T_{NI}^{G}.

The swellant nematicity has a pronounced effect on the anisotropic swelling of LCEs (Figure 2b). Parts c and d of Figure 2 show the T dependence of the degree of equilibrium swelling (Q), principal ratios ($\lambda_{||}$ and $\lambda_{\perp}$), and shape anisotropy α ($\alpha = \lambda_{||}/\lambda_{\perp}$).[24] LCE/LC solvent systems exhibit two NI transition temperatures: T_{NI}^{G} for the swollen LCE and T_{NI}^{S} for the surrounding solvent. In the totally isotropic region of $T > T_{NI}^{G}$, the LCE is highly swollen and exhibits no anisotropy. At $T < T_{NI}^{G}$, the LCE and miscible nematic swellant form a single nematic phase. In this system, T_{NI}^{N} is higher than T_{NI}^{S}; therefore, the resultant T_{NI}^{G} becomes higher than T_{NI}^{S}. The nematic ordering inside the swollen LCE at T_{NI}^{G} drives the transition from the isotropic swollen state to the nematic shrunken state having shape anisotropy elongated along the director, which is similar to the non-nematogenic solvent system. In the region of $T_{NI}^{G} > T > T_{NI}^{S}$—where the swollen LCE is in the nematic state whereas the surrounding solvent is in the isotropic state—cooling induces a reswelling; however, it is accompanied by an increase in the shape anisotropy. In the totally nematic regime of $T < T_{NI}^{S}$, the volume is almost T-independent, whereas the shape anisotropy increases with a decrease in T. The swollen LCEs in the totally isotropic and nematic regimes are similar in volume but different in shape. The anisotropic swelling and phase behaviors were thermally reversible without an appreciable hysteresis effect, and the same features were observed for the combinations of LCE and solvent with various chemical structures. These results indicate that the nematic order of nematogens plays a major role in the swelling of LCEs. This differs considerably in its governing force from the swelling of the familiar isotropic polymer networks.[25,26] The role of nematic order in swelling is more evident with the aid of a mean-field theory. Warner and Wang[27,28] proposed temperature−concentration phase diagrams for LCE/solvent systems, and they predicted the coexistence of swollen isotropic and shrunken nematic states at the NI transition point. Matsuyama et al.[29] also calculated the $T-Q$ curves including the shape change. The theoretical results fitted the data, and the corresponding theoretical order parameters are shown in Figure 2. This theory reproduces the qualitative features of the data, and it demonstrates that the swelling behavior is mainly governed by the nematic order parameter of each nematogen, i.e., S_m, S_0, and S_b for the LCE mesogen and the solvents inside and outside the LCE, respectively. Nematic ordering inside the LCE, i.e., a jump in S_m (and S_0) at T_{NI}^{G}, yields a large volume reduction as well as elongation along the director. An increase in S_m (and S_0) induces further stretching. When the surrounding nematic solvent is in the isotropic state ($S_b = 0$ at $T_{NI}^{S} < T < T_{NI}^{G}$), an increase in the nematic order inside the LCE (S_m and S_0) drives the increase in volume as well as shape anisotropy.

There are two noticeable discrepancies between the theoretical prediction and experimental observation. One is the excessive shape anisotropy in the former. This arises from the overestimation of S_m by the Maier−Saupe approach. The S_m data for the swollen LCE immersed in solvent is not obtained due to experimental difficulties; however, the actual value of S_m will be considerably less than the expected value.[30] The other and more important discrepancy is that transitions at T_{NI}^{G} in the experiments occur smoothly without the discontinuities expected from the first-order phase transition. The continuous change in both the order parameter and strain at the

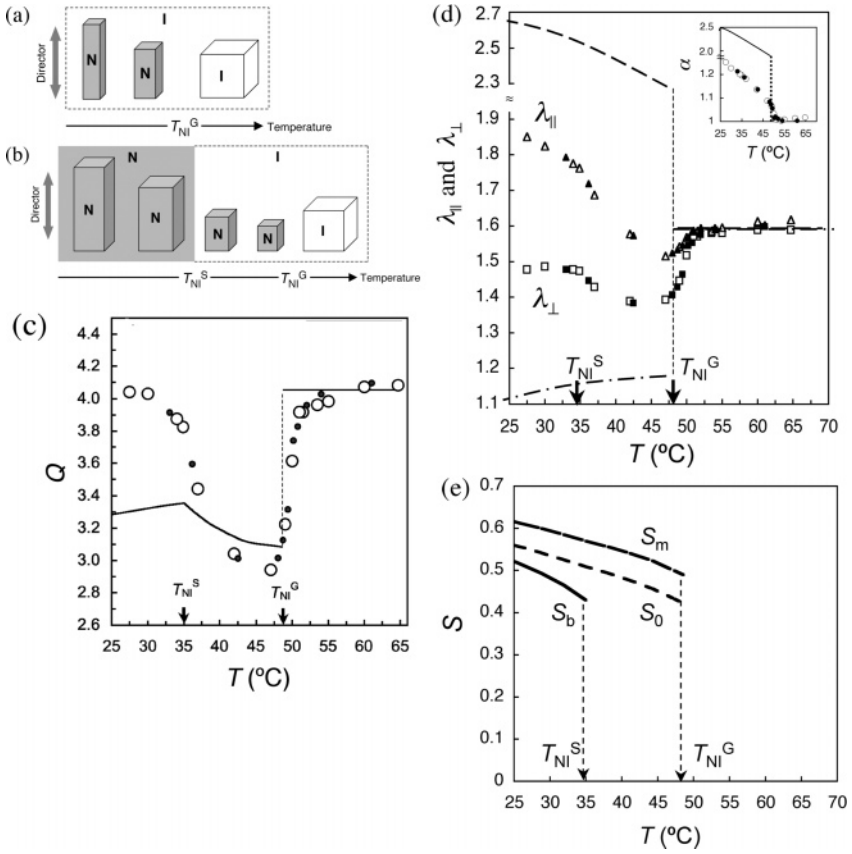

Figure 2. Schematic diagrams of the temperature (T) dependence of equilibrium volume and shape of a monodomain LCE swollen in (a) nonmesomorphic solvents and (b) low-molecular-mass LCs. The temperatures T_{NI}^G and T_{NI}^S are the nematic−isotropic (NI) transition temperatures of the swollen LCE and surrounding pure LC solvent, respectively. (c) The degree of equilibrium swelling (Q). (d) Principal ratios (λ) parallel (||) and normal ($\perp$) to the director, and shape anisotropy (α: $\alpha = \lambda_\perp/\lambda_{||}$) of a monodomain LCE with the mesogen MP immersed in the LC solvent 5CB (Figure 1) as a function of temperature. The cross-linker concentration in the feed is 7 mol %. The open and filled symbols represent the data on cooling and heating, respectively. The principal ratios are defined as $\lambda = l/l_{dry}^I$, where l and l_{dry}^I are the dimensions along the corresponding axis in the fully swollen, dry and isotropic states, respectively. The degree of swelling (Q: $Q = \lambda_{||}^2\lambda_\perp$) is the volume ratio in the dry and swollen states. The lines depict the fitted theoretical results. (e) The temperature dependence of order parameters (S) obtained by the fitting of the theoretical prediction to the swelling data. The parameters S_m, S_0, and S_b are for the LCE mesogen and the solvents inside and outside the LCE, respectively. The data are reproduced from ref 24.

transition has already been observed for neat monodomain LCEs in many studies,[5] and the results shown in Figure 2 confirm that smooth NI transition also occurs in the swollen state. Why is the NI transition of monodomain LCEs smooth unlike that of the usual nematics? There is an ongoing dispute between two radically different explanations about this issue. The first explanation is that the discontinuity vanishes because of a supercritical effect caused by an aligning stress, such as liquid−gas transition under high pressures, beyond a critical value.[1,31−34] The aligning stress may arise from stress applied on the sample and/or internal stress arising from cross-linking in the nematic state. The second explanation attributes the smooth transition to the broadening of the transition originating from heterogeneity in the network structures or local nematic order.[35,36] A theoretical study[37] has argued that quenched orientational disorder stemming from the presence of cross-links adds a S^{-4} energy term to the Landau−de Gennes expression and that it reduces the first-order discontinuity at the transition. An important aspect of this issue is that swollen polydomain LCEs exhibit a definite jump in volume at T_{NI}^G with an expected first-order discontinuity.[24,38,39] This issue is further described in section 5.

With regard to the swelling and phase behavior of LCEs, the theoretical studies appear to be more advanced than the experimental studies. Several theoretical studies have pointed out the following factors that significantly influence the behavior of swollen LCEs: (i) the relative nematicity of LCE and solvent,[28,29] (ii) the strength of nematic cross-coupling between LCE and solvent,[28,40] and (iii) external fields (such as mechanical stress[28] and magnetic[29] and electric fields) that affect the nematic order. For (i), almost symmetrical phase diagrams for the systems of $T_{NI}^G > T_{NI}^S$ and $T_{NI}^G < T_{NI}^S$ are theoretically expected; however, this has not yet been proved due to lack of available data for the latter system. In principle, the latter system can be realized if we employ a strong nematic solvent or weak nematic network to satisfy the condition of $T_{NI}^S > T_{NI}^N$. For (ii), the studies on un-cross-linked LC polymer/nematic solvent systems[41,42] have shown that the strong cross-interaction between some combinations of dissimilar mesogens stabilizes the single nematic phase formed by the mixtures, and the resultant T_{NI} value can become greater than both the transition temperatures of the pure components although the T_{NI} values of usual nematic mixtures lie between them. In swollen LCEs, the strong cross-interaction is considered to have a significant effect on not only T_{NI}^G but also the volume and shape of LCEs in the nematic state. For (iii), an imposed field affecting the nematic order would shift the swelling and phase equilibria and also change the volume and shape. The experimental characterizations for issues (i)−(iii) will reveal some new and important features regarding the coupling of nematic order with volume and shape. Further, it should be noted that the effect of smectic ordering on swollen LCEs has been investigated neither theoretically nor experimentally.

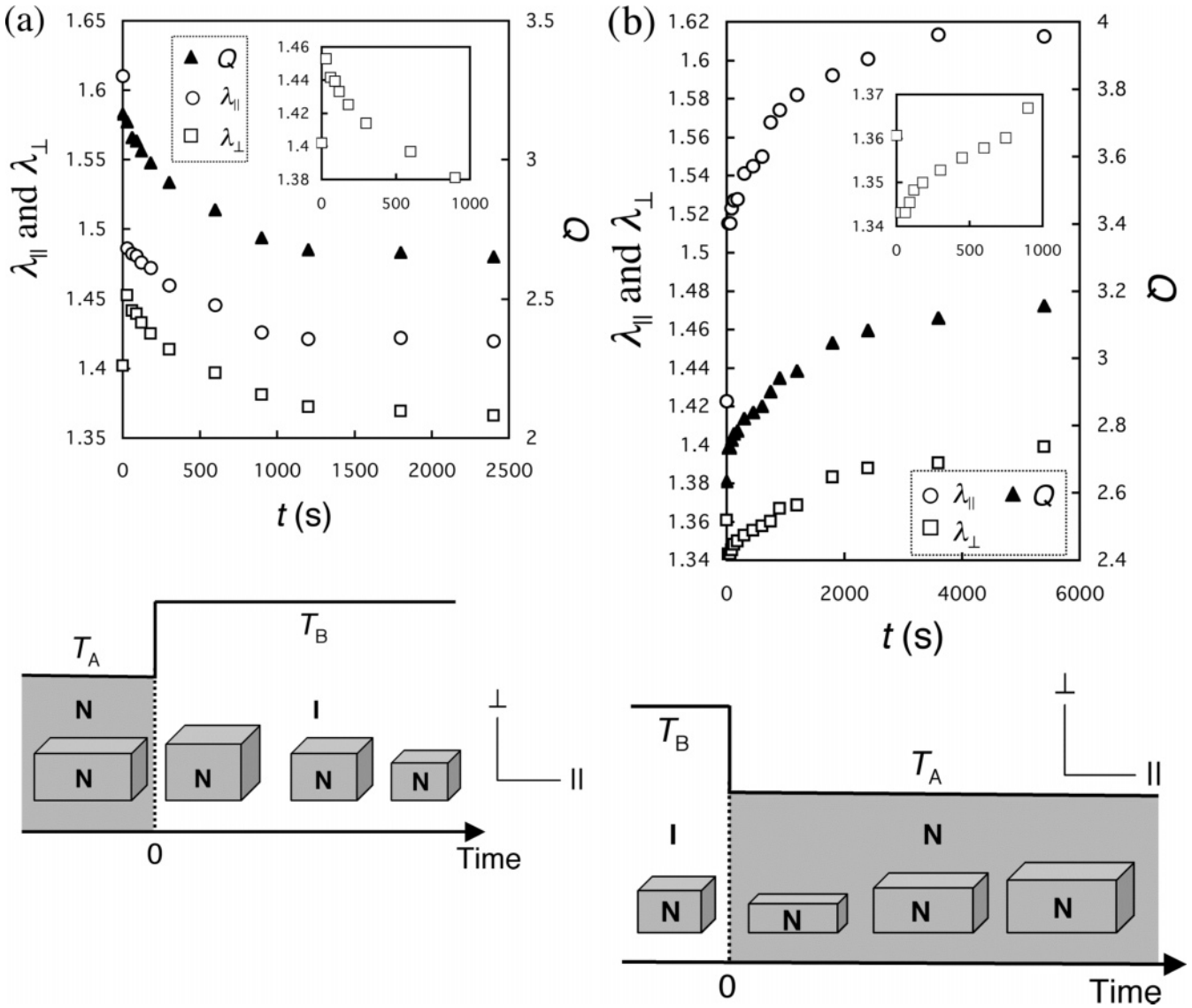

Figure 3. Principal ratios (λ) in the directions parallel (||) and normal ($\perp$) to the director, and the degree of swelling (Q) as a function of time (t) after T-jumps of (a) $T_A \rightarrow T_B$ and (b) $T_B \rightarrow T_A$, where T_A and T_B belong to the totally nematic region ($T_A < T_{NI}^S$) and the region between T_{NI}^S and T_{NI}^G ($T_{NI}^S < T_B < T_{NI}^G$), respectively. The LCE is the same as that in Figure 2, and the nematic swellant is 7CPB (Figure 1). The insets show $\lambda_\perp(t)$ in a short-time region. Schematic diagrams of (a) the shrinking process with the overshoot of $\lambda_\perp$ and (b) swelling process with the undershoot of $\lambda_\perp$. The dimensional and volume variations in the figure are enlarged for explanation. From ref 43.

The swelling and shrinking of LCEs also exhibit unusual features in their dynamic characteristics.[43] Parts a and b of Figure 3 show the time (t) dependence of λ and Q during shrinking and swelling after the T-jumps between T_A and T_B, respectively; here, T_A and T_B belong to the totally nematic region ($T_A < T_{NI}^S$) and region between T_{NI}^S and T_{NI}^G ($T_{NI}^S < T_B < T_{NI}^G$), respectively. The equilibrium values of $\lambda_{||}$, $\lambda_\perp$, and Q are greater at T_A than at T_B, as observed in Figure 2b. The times required for the T-jumps are negligible (less than 10 s) as compared to the time scale of interest. Importantly, $\lambda_\perp(t)$ exhibits a pronounced overshoot or undershoot behavior during the shrinking or swelling process, respectively, whereas the volume changes show no noticeable anomaly. These results clearly reveal that the swelling and shrinking dynamics of monodomain LCEs comprise shape and volume variation modes with significantly different characteristic times.[44] The former induces a rapid compression or elongation along the director that occurs simultaneously with the T variation with decrease or increase in S, respectively. The latter induces a volume variation—a slow process governed by the diffusion of polymer networks such as the swelling of isotropic gels.[45−47] The dimensional overshoot and undershoot occur in a direction normal to the director, where the effect of shape variation on the dimension opposes that of volume variation. Along the director direction where these two effects on the dimension synchronize, a large change (more than 50% of the total change) occurs immediately after the T-jumps. Kinetic theories have been developed to describe the swelling of isotropic networks.[45−47] The theoretical modeling of the anisotropic swelling dynamics of nematic networks comprising two different modes is a challenging issue.

4. Deformation Coupled with Director Realignment

In most of the earlier studies, the director reorientation by external fields was studied by employing mechanical stretching imposed normal to the initial director.[49−54] A sufficiently large strain (stress) can cause a full director rotation by 90° along the field axis. However, in mechanical stretching, a globally uniform shear deformation is not possible because of clamps holding the sample at both the ends. Consequently, the induced director realignment often becomes nonuniform. The formation mechanism of the characteristic inhomogeneous (stripe-domain) patterns of director reorientation has been theoretically

investigated.[55−57] The deformation mode that occurs during globally uniform director rotation is also an important and fundamental issue in the physics of LCEs.[3,5,58,59] However, it has not been characterized because of experimental difficulties in realizing full director rotation in LCEs without external constraints. In section 4.1, we show that such a deformation mode can be achieved through the electric field response of swollen LCEs that are not mechanically constrained in optical cells. In section 4.2, we introduce some interesting patterns of director realignment (other than the above-mentioned stripe-domain pattern) that are caused by frustration in constrained LCEs.

4.1. Deformation Induced by Director Rotation in Unconstrained Geometry. As is well-known by electrooptical effects in low-molecular-mass LCs, nematogen realignment can be achieved by low electric fields because of their large dielectric anisotropy and nematic interaction. In (solid) LCEs, the electrically induced mesogen realignment drives macroscopic distortion. The mechanism of this electrical deformation of LCEs differs from that of other familiar electrical deformations such as electrostriction and inverse piezoelectricity. The electrical deformation of (paraelectric) LCEs based on dielectric anisotropy leads to an interesting feature; dielectrically positive or negative LCEs—where the dipole moment of the mesogen is parallel or normal to its long axis—are macroscopically stretched in a direction parallel or normal to the field axis, respectively.[60] However, in the neat state, unusually high field strengths were required to achieve a finite deformation because the high elastic moduli act as a strong resistance to the dielectric realigning force.[61,62] The swelling in low-molecular-mass LCs decreases the network modulus without decreasing the dielectric anisotropy, and it facilitates the actuation of LCEs under moderate field strengths.[20−22,60,63−65] Polydomain LCEs in such a swollen state exhibit a finite electrical deformation; however, the characterization of the induced mesogen realignment is difficult owing to their stacked mosaic texture.[60] A full 90° rotation of the director and induced distortion are visible in swollen monodomain LCEs under unconstrained geometry.[64]

Figure 4a shows the response of an unconstrained swollen LCE with positive dielectric anisotropy to an electric field (*z*-direction) normal to its initial director (*x*-direction).[64a] The electric field drives the anisotropic deformation as well as a large decrease in birefringence in the $x-y$ plane as a result of director realignment along the *z*-axis. Figure 4b displays the electrically induced strains (γ) in the *x*- and *y*-directions and the effective birefringence in the $x-y$ plane (Δn_{eff}) as a function of voltage amplitude of the sinusoidal field between electrodes (V_0). A strong correlation between a change in Δn_{eff} and γ_x is evident in the figure. Almost complete director rotation toward the field direction ($\Delta n_{\mathrm{eff}} \approx 0$) is achieved by sufficiently high fields (ca. 20 V/μm). The induced deformation primarily occurs in the plane of director rotation. The compressive strain γ_x (<0) along the initial director axis exceeds 15% at high fields for a loosely cross-linked LCE (Figure 4d), whereas almost no distortion is observed along the *y*-direction. Since LCEs are mechanically incompressible, γ_z is extensional and has a magnitude similar to γ_x. Another observation from a different angle confirmed that the dielectrically positive LCEs used here are stretched along the field axis.[60] Figure 4c shows a schematic diagram of the deformation induced by a 90° rotation of the director. This is the pure shear deformation where the specimen is uniaxially stretched but without lateral shrinkage in one direction. This anisotropic deformation is also characterized by the Poisson ratio (μ) as $\mu_{xz} \approx 1$ and $\mu_{yz} \approx 0$ when the distortion is considered to be uniaxial stretching along the *z*-direction. This is in contrast to $\mu_{xz} = \mu_{yz} = 1/2$ for incompressible isotropic elastomers. The deformation and the transmittance change are repeatable when reiterating the application and removal of the fields. The time required to response to "field on" was evaluated to be ca. 5 ms on the basis of the change in Δn_{eff} upon the application of the field of $V_0 = 400$ V and $f = 1$ kHz. The force generated by this distortion (ca. 10% strain) is not directly measured; however, we crudely estimate it to be of the order of 10^3 Pa from the modulus of the LCE film (ca. 0.02 MPa).

What is the pathway between the two states ($\theta = 0°$ and 90°) in Figure 4c like? The angle θ is the rotation angle of director, and $\theta = 0°$ and 90° correspond to the initial state and complete rotation along the field axis, respectively. Figure 4d illustrates γ as a function of θ for the specimens with different cross-linker concentrations (C_x) where θ was evaluated from the data of Δn_{eff}.[64b] The soft elasticity theory[3,5,58,59] proposes that the pathway from $\theta = 0°$ to 90° consists of pure shear deformation and body rotation, as schematically shown in Figure 5a. The variation in θ from 0° to 90° results in stretching along the rotated director and compression along the initial director axis without dimensional changes along the *y*-direction. The expression of $\gamma_i(\theta)$ in this model[59] for a sufficiently thin film specimen ($l_z^\circ \ll l_x^\circ$) is given by[64b]

$$\gamma_x = -\left(1 - \frac{1}{k}\right)\sin^2\theta \tag{1a}$$

$$\gamma_y = 0 \tag{1b}$$

$$\gamma_z = (k-1)\sin^2\theta + \frac{l_x^\circ}{l_z^\circ}\left(1 - \frac{1}{k}\right)\sin\theta\cos\theta \tag{1c}$$

where *k* is a measure of the shape anisotropy of polymer chains arising from the nematic order and l_x° and l_z° are the dimensions measured along the *x*- and *z*-directions at $\theta = 0°$, respectively. The theory typically considers γ_x to be proportional to $\sin^2\theta$ and $\gamma_y = 0$ to be independent of θ, which is in good agreement with the data for all the specimens, as shown in Figure 4d. However, some discrepancies can be observed in the other features. First, in the experiments, a considerable body tilting is absent during the intermediate stage of director rotation at $\theta \approx 45°$ (Figure 5b). The maximum tilt angle ω ($\tan\omega = l_x/l_z$) is as small as a few degrees; however, the specimen cannot tilt remotely from the electrodes because the resulting l_z value is considerably greater than the gap between the electrode and sample. The resultant contact of the specimen with the transparent electrodes was not observed by optical microscopy. Second, the C_x dependence of *k* evaluated from Figure 4d shows an opposite trend to that obtained from swelling anisotropy ($\alpha = k$),[17] although the *k* values evaluated by these two independent methods are similar in magnitude,[64b] as shown in the inset of the figure. Real systems exhibit an anchoring effect on the specimen surface and/or surface tension effect, none of which is considered in the theory. In addition, the soft elasticity theory originally proposes that full director rotation does not consume energy in ideal LCEs without either the anchoring effect or chain-entanglement effect.[3,5,66,67] In the experiments, a high external field is required to achieve full director rotation, and recovery to the initial state rapidly occurs upon field removal. This indicates that real systems are not purely soft. Nevertheless, it is noteworthy that the theory reproduces the most characteristic results: $\gamma_x(\theta) \sim \sin^2\theta$ and $\gamma_y(\theta) \approx 0$. The deformation mode in the process of full director rotation provides an important basis to understand the coupling of the rubber elasticity and

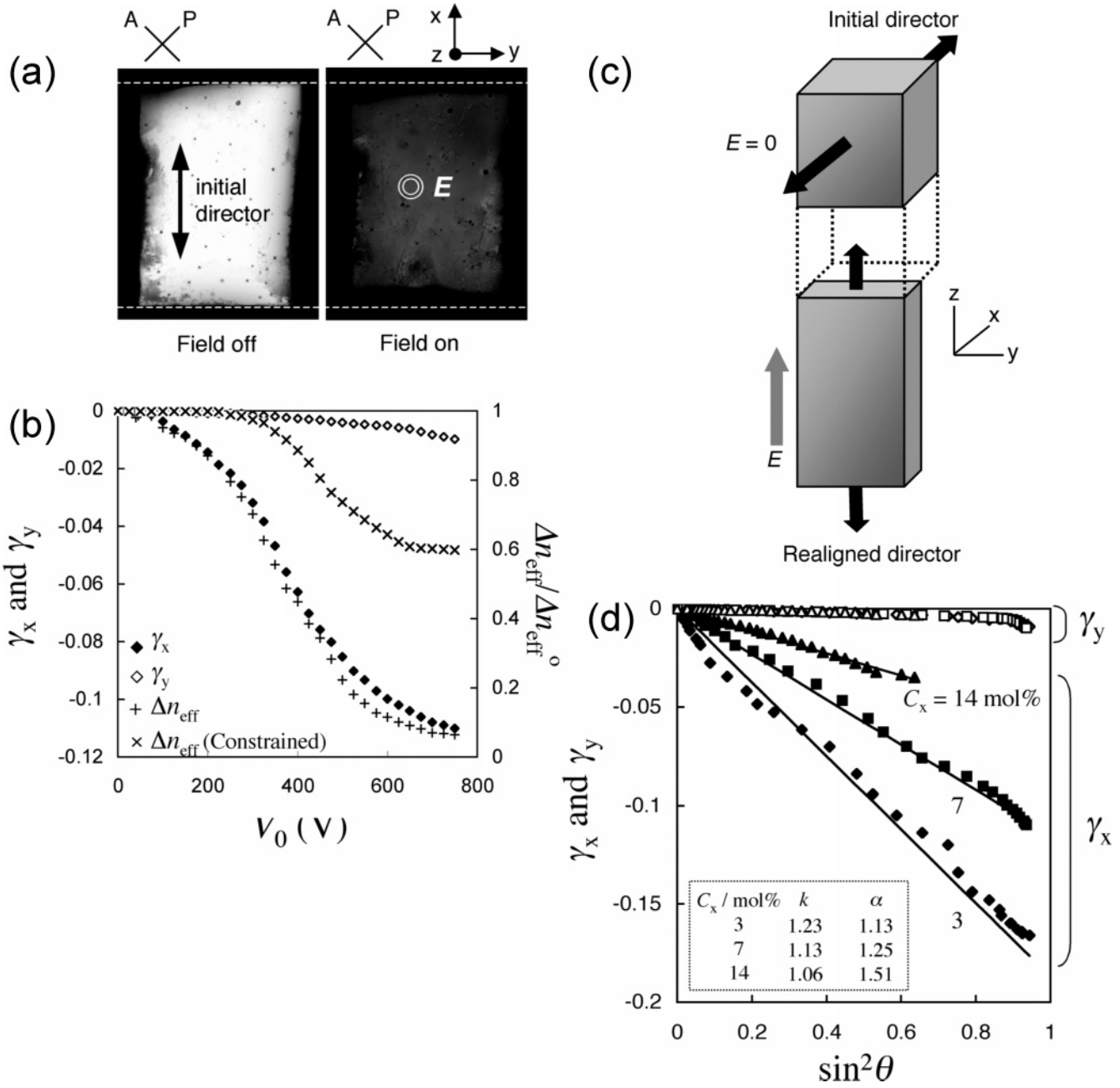

Figure 4. (a) Electrooptical and mechanical effects in a dielectrically positive monodomain LCE swollen by 5CB (Figure 1) in unconstrained geometry at 25 °C. The sample is the same as that in Figure 2. A and P denote the optical axes of the analyzer and polarizer, respectively. The sinusoidal voltage $V_0 = 750$ V at 1 kHz is imposed normal to the initial director (*x*-direction). The gap between electrodes (40 μm) is greater than the film thickness (34 μm), and the cell is filled with a transparent silicone oil (nonsolvent for the LCE) such that the specimen is not mechanically constrained by the electrodes. The field drives director realignment along the field axis (*z*-direction) that is indicated by a large decrease in birefringence in the $x-y$ plane and simultaneous anisotropic deformation of ca. 10% compression along the *x*-direction but without any appreciable dimensional change along the *y*-direction. From ref 64a. (b) The strains γ_x, γ_y and effective birefringence Δn_{eff} in the $x-y$ plane as a function of apparent voltage amplitude (V_0) between the electrodes. The strains γ_i is defined by $\gamma_i = (l_i - l_i^\circ)/l_i^\circ$, where l_i and l_i° are the specimen dimensions measured along the *i*-axis in the deformed and undeformed states, respectively. The birefringence is reduced by the initial values at $V_0 = 0$. The sample is the same as (a). The data of Δn_{eff} of the same specimen effectively sandwiched by electrodes ($\gamma_z = 0$) are also shown. The data are reproduced from ref 64b. (c) Schematic diagram for the distortion induced by a 90° rotation of the director. The induced deformation is pure shear where the specimen is stretched along the realigned director but without lateral shrinkage in the direction irrelevant to the director rotation. (d) The strains γ_x and γ_y as a function of $\sin^2\theta$, where θ is the director rotation angle evaluated from Δn_{eff} for the samples with different C_x. The inset compares the shape anisotropy parameters *k* and α that are evaluated from the θ dependence of γ_x (eq 1a) and the anisotropy in swelling, respectively. The data are reproduced from ref 64b.

mobile director. A complete understanding of this deformation mode will require further development of the theory and detailed characterization.

4.2. Fréedricksz Effect and Buckling Distortion in Constrained Geometry. The constrained geometry that prohibits the strain in one direction significantly suppresses the director realignment in the corresponding direction. Figure 4b shows a comparison between the electrooptical effects of a swollen LCE in the unconstrained state and that of an LCE effectively sandwiched by electrodes ($\gamma_z = 0$).[64b] In the constrained state, the reduction in Δn_{eff} saturates at high fields, and the total decrease from the initial value is only 40%. This is considerably less than the decrease of ca. 95% in the unconstrained state. Further, the threshold field for the onset of director rotation in

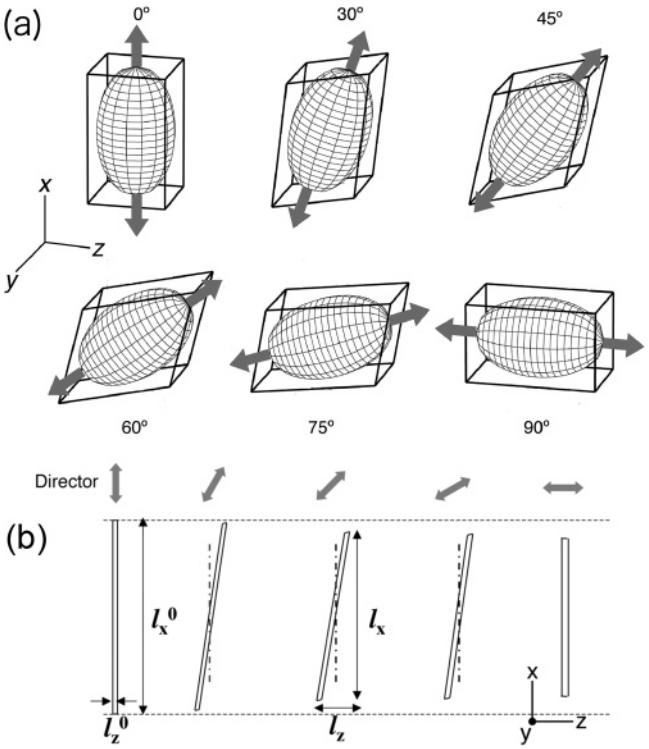

Figure 5. (a) Schematic depiction of soft deformation pathway during a 90° rotation of the director for small volume elements having the anisotropy of $k = 1.67$. The arrows indicate the director direction. The deformation is composed of pure shear and body rotation. Figure courtesy of M. Warner. (b) Macroscopic deformation in the $x-z$ plane for the thin LCE film with $l_x°/l_z° = 40$ and $k = 1.34$ on the basis of eq 1. From ref 64b.

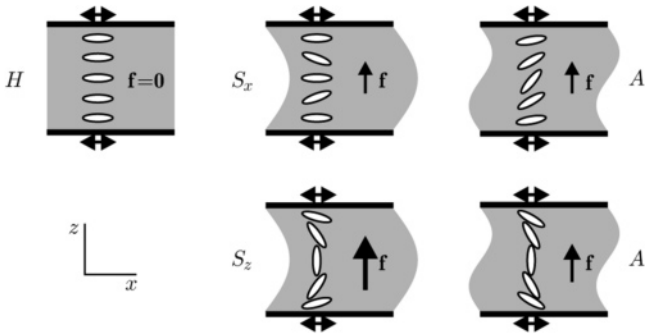

Figure 6. Schematic depiction of configurations in a constrained LCE under a normal external field *f*. In the absence of the field, the homogeneous alignment *H* is observed. In weak fields, the antisymmetric configuration *A* or symmetric configuration S_x is observed depending on the nematicity and film thickness. In strong fields, the symmetric S_z structure is formed. Reprinted with permission from ref 71. Copyright 2006 EDP Sciences.

the constrained state is ~1 order of magnitude greater than that in the unconstrained state. These results evidently indicate that the director reorientation is strongly suppressed, and a full 90° rotation of the director never occurs in this constrained geometry.

What type of mesogen reorientation occurs in the constrained geometry? The electrooptical effect of monodomain nematic networks (formed in the presence of a considerable amount of LC solvent inside the optical cell) in this geometry has been studied by several researchers.[68−70] Conoscope observations have revealed an S_x-type (Figure 6) alignment; further, it is considered that the shear in the sample plane is also apparent from the translation of dust and other imperfections imbedded in the gel.[70] The S_x structure accompanying the shear strain is significantly different from the *A*-type structure (Figure 6) that is similar to the conventional Fréedericksz effect of nematics. The *A*-type structure exhibits half the wavelength of director rotation between the plates, whereas the S_x structure in LCEs exhibits the full wavelength. This difference originates from the fact that LCEs exhibit rubber elasticity in addition to the Frank elasticity of LCs.[70] The director in LCEs (solid) is anchored by the matrix itself, whereas that in usual nematics (liquid) is anchored only at the substrate surfaces. The difference is also evident from the fact that the threshold for the onset of director response in LCEs is determined by the field strength rather than the voltage, unlike in usual nematics.[64b,69,70] However, a considerable amount of study is still required to investigate the various aspects of the Freedericksz effect. Detailed measurements revealing either the overall deformation or the shear gradient are absent. The direct observation of the $x-z$ plane is required to reveal the induced distortion. Further, in refs 70 and 71, it is considered that the crossover from the S_x structure to the *A* structure might occur when the thickness of LCEs decreases to a characteristic length as a result of the merging of the two nonuniform regions and the boundary wall domain. A qualitative observation of such crossover behavior has been mentioned in ref 70, but the onset thickness for this transition has not been characterized. Further, a Monte Carlo simulation[71] suggests that sufficiently high fields can result in S_z structures where the director is aligned along the field axis even in the central layer of the sample. A theoretical study[72] also suggests that a Fréedericksz or undulation instability occurs at the onset of the director response depending on the sample thickness and material parameters. Thus, the experimental characterization of the influences of various parameters (including network modulus and nematic order) on the Fréedericksz effect remains incomplete.

Another interesting phenomenon is the buckling deformation of a monodomain nematic gel (formed in the optical cell) constrained by glass plates that occurs upon cooling in the low-temperature nematic phase,[73] as shown in Figure 7. The cooled gel becomes significantly frustrated because its expansion, which is to be induced along the director, is prevented by the boundary conditions. The buckling distortion represents a low-energy deformation incorporating a periodic strain field coupled with periodic rotations of the director. This deformation mode decreases the rubber elastic energy to a greater extent than the undeformed state at the cost of a Frank elasticity penalty. It was also revealed that the pitch of the striped texture is larger in weaker nematic gels with thicker phase gaps, and the stripe is absent in nematic gels that are extremely thin or weak. The pitch characteristics arise from the competition between the nematic rubber elasticity and Frank elasticity of LCs. It is important to study the thermally induced spontaneous deformation of the same sample in the unconstrained state in order to interpret quantitatively the buckling deformation in the constrained state. Unfortunately, the gel employed was too soft to perform experiments in the unconstrained state. A similar type of striped texture can also be possibly observed in conventional LCEs with sufficiently high moduli. A systematic study of constrained and unconstrained geometries for LCEs with various nematicities and thickness values will reveal the details of the coupling of the rubber elasticity with the Frank elasticity. Further, another type of mechanical constraint or director realignment may cause different types of frustration in LCEs that result in new inhomogeneous orientation patterns.

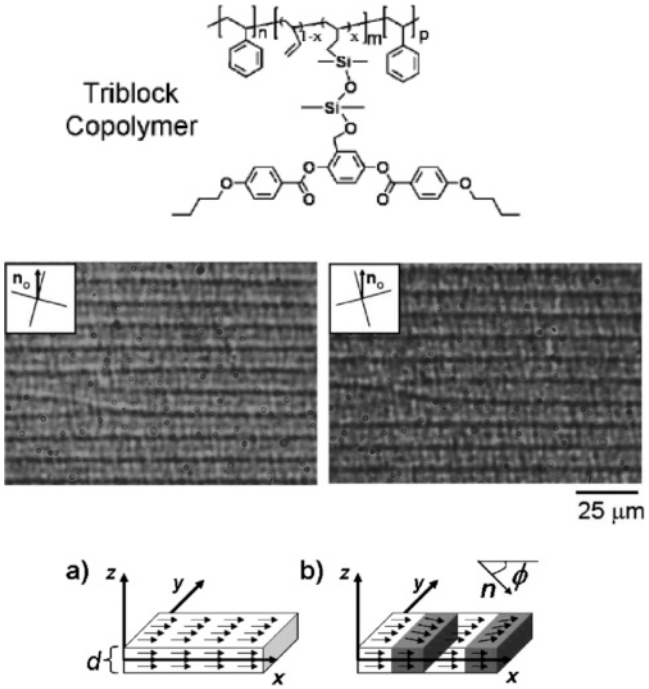

Figure 7. An LC gel confined in a cell when cooled to 25 °C from 35 °C observed with a polarizing optical microscope. The LC gel is formed by the self-assemblage of a polystyrene−side-chain LC polymer−polystyrene triblock copolymer dissolved in 5CB (Figure 1). The less soluble polystyrene block aggregates to form physical cross-links. The orientation of the director imprinted during cross-linking n_0 and the orientation of the crossed polarizers is shown in the top left-hand corner of each image. The dark lines in the left-hand image become bright in the right-hand image, and vice versa. Director alignment in (a) the initial uniformly aligned state and (b) the buckling deformed state. The cell substrates are at $z = \pm d/2$. Reprinted with permission from ref 73. Copyright 2006 American Physical Society.

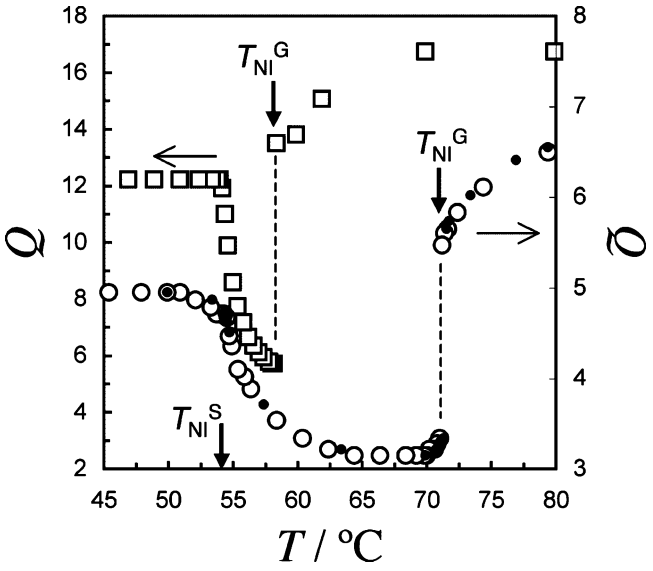

Figure 8. Degree of equilibrium swelling (Q) as a function of temperature for the two polydomain LCEs composed of MP (○) and MN (□) (Figure 1) swollen by the nematic solvent 7CPB. The temperatures T_{NI}^{G} and T_{NI}^{S} denote the NI transition temperatures of the swollen LCEs and pure surrounding solvent, respectively. The open and filled symbols denote the data obtained on cooling and heating, respectively. Note that the volume changes at T_{NI}^{G} are discontinuous. The data are reproduced from ref 83.

5. Nematic Elastomers and Gels Having Disordered Directors

As mentioned in section 2, if the mesogen alignment is untreated at the cross-linking, the resultant LCEs have a disordered polydomain texture without a global director. Polydomain LCEs have attracted considerably less interest than monodomain LCEs because of the absence of anisotropy in their macroscopic properties. Polydomain structures characterized by Schlieren texture in usual nematics may be regarded as the kinetic effect of a macroscopically aligned equilibrium state. In contrast, polydomain textures in LCEs appear to be a thermodynamic equilibrium state, where the Frank elasticity is balanced by the disordering force due to the defects (cross-links) quenched in the networks.[74,75] In recent years, LCs with quenched disorder characteristics such as nematics embedded in the disordering host structure (for example, random porous media) have received considerable attention because of numerous interesting properties.[76−78] Polydomain LCEs significantly differ from such disordered LC systems in terms of the source and length scale of the random disorder.[79] The quenched disorder in the latter arises from the anchoring of the random porous media on the surface, and the domain size of the resultant texture is similar to or smaller than the source size. The main sources of quenched disorder in the former are the cross-links and defects in the network structure, and each local domain in the order of microns contains many cross-links. In addition, polydomain LCEs are similar to spin glasses and random magnets in terms of the spatial correlations of alignments because they are composed of randomly oriented local domains and have no overall alignment.[79] A familiar phenomenon of polydomain LCEs is the polydomain-to-monodomain (P−M) transition induced by elongation.[74,80−82] A considerably low uniaxial stress drives the transition from the disordered director texture to a globally aligned state. The P−M transition has been discussed in detail in earlier studies.[5−7] Here, we describe phase transition, swelling behavior, and slow dynamics specific to polydomain LCEs.

5.1. Phase Transition and Swelling Behaviors. Figure 8 show the T dependence of equilibrium swelling for the polydomain LCEs composed of different mesogens (MP and MN) in a low-molecular-mass LC.[38,83] Two important issues arise when the behaviors of monodomain (Figure 2) and polydomain LCEs are compared. The swelling of polydomain LCEs exhibits no anisotropy ($\alpha = 1$) owing to the absence of a global director, unlike the anisotropic swelling of monodomain LCEs. However, they exhibit a similar T dependence of macroscopic volume Q, particularly with regard to the reentrant dependence (reswelling behavior on cooling) in nematic solvent systems. This indicates that the action of the local nematic order on the overall volume is equivalent to that of the globally aligned nematic order. It appears that each local domain independently swells in a similar manner to monodomain LCEs such that there is neither connectivity nor correlation between the different domains. This may be possible if the osmotic bulk modulus is considerably greater than the shear modulus;[84] however, the mechanism of similarity in the $T-Q$ behavior between polydomain and monodomain LCEs remains unclear.

Most importantly, polydomain LCEs exhibit a discontinuous volume change during the NI transition in accordance with the expected first-order transition, which is in contrast with the smooth NI transition in monodomain LCEs. Why are their NI transitions so different? It is perplexing that the two existing scenarios for the smooth transition in monodomains (see section 2) appear to explain the discontinuous transition in polydomains. The polydomain texture is formed in the actual thermodynamically equilibrium state. The polydomain LCE have neither applied stress nor internal stress aligning the mesogens during

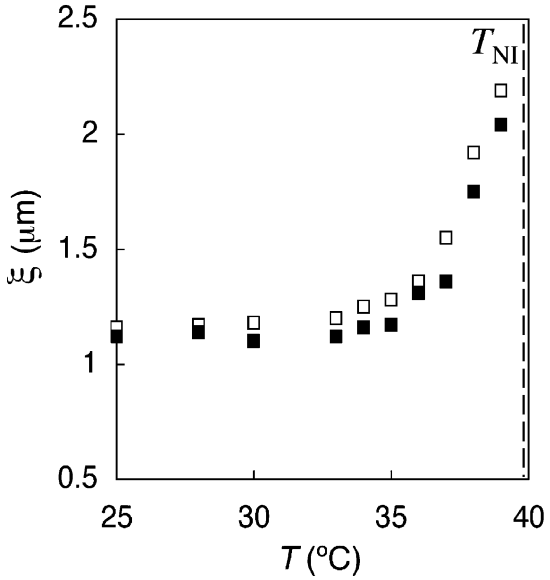

Figure 9. Temperature dependence of the characteristic texture size (ξ). The data are extracted from light-scattering studies[75] on a side-chain polydomain LCE based on siloxane backbone in the neat state. Open and filled symbols denote the data obtained on heating and cooling, respectively. The data are reproduced from ref 5.

cross-linking. In addition, they do not have a spatially large heterogeneity formed upon cross-linking in the artificially achieved monodomain state. If the macroscopic size of a monodomain LCE is decreased to a few micrometers, which is similar to the local domain size of polydomains, does such a small monodomain system exhibit a sharp transition? An experiment regarding this question will be a critical test for the existing explanations.

Few measurements of the domain size (ξ) of polydomain LCEs have been conducted.[75] It has been demonstrated that ξ rapidly increases in the vicinity of T_{NI} when $T \rightarrow T_{NI}$ (i.e., as the local nematic order S decreases), as shown in Figure 9. The evolution of ξ near T_{NI} was expressed as $\xi \sim (T_{NI} - T)^{-y}$ with $y = 1$. The domain size is determined by a balance between the Frank elasticity and random disordering effect. The evolution of ξ near T_{NI} implies that a decrease in S causes a larger reduction in the latter effect than in the former. A similar behavior of ξ near T_{NI} is observed in un-cross-linked LC polymers in the polydomain state.[85] Several theoretical papers[79,86,87] studied the determinant of ξ; however, the effects of temperature and cross-linking are still unclear. In order to elucidate the transition behavior of polydomain LCEs, we require further information, in particular, about the local nematic order for polydomains. Probably, only NMR measurements are accessible,[88] but no data for polydomain LCEs have been reported.

5.2. Effects of Cross-Linking History. Polydomain LCEs can be obtained via two different routes. The first is by cross-linking the mesogenic monomers in the low-temperature polydomain nematic state. The second is by cross-linking the mesogens in the high-temperature isotropic state and cooling the resultant networks to the low-temperature nematic state. Several studies have examined the properties of the former and/or latter LCEs (designated as N-PLCE and I-PLCE, respectively);[80,82] however, most of them did not focus on the effect of cross-linking history. These two LCEs with the same cross-linker concentration exhibit no appreciable difference in the equilibrium properties such as T_{NI}^{N}, T_{NI}^{G}, and Q,[80,89] as shown in the inset in Figure 10a. This implies that the mesogen alignment in the cross-linking stage does not appreciably affect

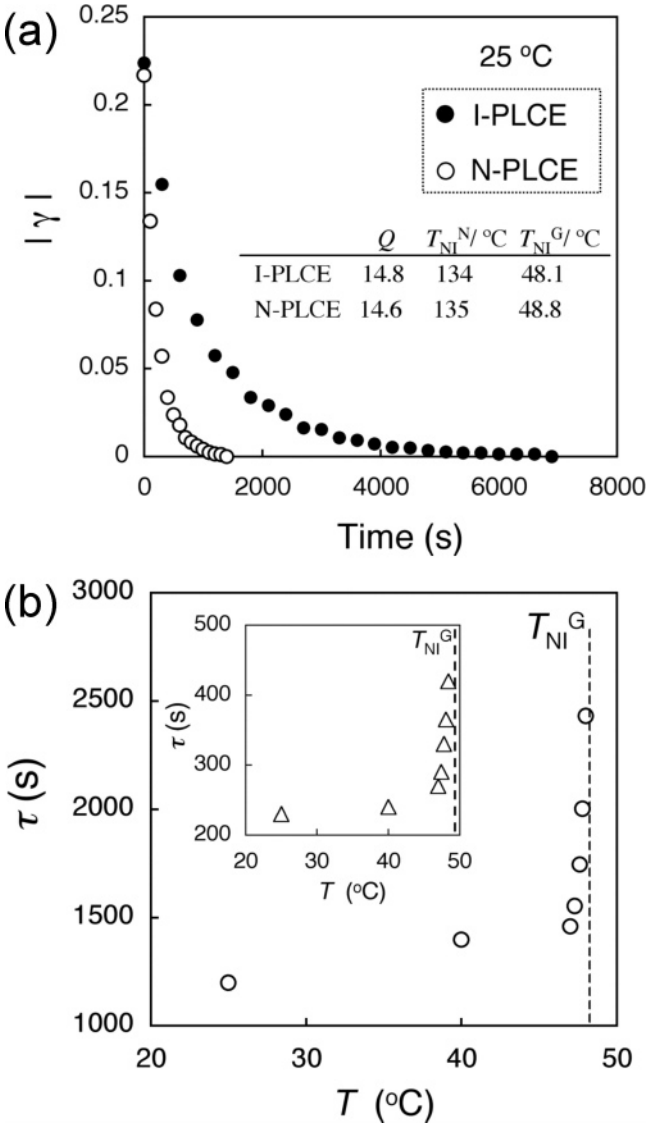

Figure 10. (a) Time dependence of γ during the shape recovery of the swollen polydomain LCEs (I-PLCE and N-PLCE) with a cross-linker concentration of 1 mol % at 25 °C. The LCE mesogen and swellant are MP and 5CB (Figure 1), respectively. The data at $t = 0$ corresponds to the strain induced by the applied field (γ_0). The characteristic times for I-PLCE and N-PLCE are 1.4×10^3 and 2.6×10^2 s, respectively. (b) Temperature (T) dependence of the characteristic time (τ) of I-PLCE. The inset figure is for N-PLCE. The NI transition temperatures T_{NI}^{G} of I-PLCE and N-PLCE are 48.1 and 48.8 °C, respectively. The data are reproduced from ref 89.

the nematic order of the local domains in the resulting polydomain LCEs. In contrast, they significantly differ with regard to the dynamic features. Figure 10a shows the strain recovery of I-PLCE and N-PLCE with the same cross-linker concentration after an imposed electric field was removed at $t = 0$.[89] There is no appreciable difference in the field-induced static strain at $t = 0$. A slow shape recovery is observed on the order of 10^3 s. These slow dynamics primarily arise from the polydomain nature rather than the viscoelastic relaxation due to chain-entanglement effects because a monodomain LCE exhibits a fast shape recovery within 1 s. The slow dynamics of polydomain LCEs were also observed in slow stress relaxation during P−M transition.[90] Importantly, the characteristic time (τ) for the shape recovery of I-PLCE is ca. 5 times greater than that of N-PLCE. This result indicates that the initial director alignment upon cross-linking in the polydomain texture is memorized by the resultant network (N-PLCE); further, this

memory effect yields a strong disorder correlation to accelerate the recovery from the oriented state to the initial state. It is also noteworthy that these strain recovery processes obey an exponential-type function rather than a stretched exponential function and power law that are often employed to describe the slow dynamics of random disordered systems. A theoretical study[87] showed that the effect of cross-linking history also emerges in the stretching-induced P−M transition, whereas no corresponding experimental survey has been conducted thus far.

The shape recovery of I-PLCE and N-PLCE becomes considerably slower near T_{NI} when $T \rightarrow T_{NI}$,[89] as shown in Figure 10b. The T dependence of τ near T_{NI} is expressed as $\tau \sim (T_{NI} - T)^{-x}$ with $x = 0.2$ for both the LCEs. This deceleration implies that the magnitude of the induced reduction in the elastic restoring force is larger than that in the viscous resistant force when the local nematic order decreases. The increase in τ near T_{NI} should be related with the evolution of ξ (Figure 9), but the correlation is unclear. Much remains unknown about the static and dynamic aspects of polydomain LCEs.

6. Summary and Outlook

We have described some select issues on LCEs and LC gels arising from recent researches. When globally aligned monodomain LCEs are immersed in a solvent, the nematic order couples both volume and shape and they behave as the anisotropic gels with *T*-responsive volume and shape. This reveals some new aspects in the swelling and/or phase behavior that are absent in non-nematogenic network/solvent and uncross-linked LC polymer/solvent systems. The existing theory qualitatively explains the anisotropic swelling behavior that is primarily governed by the nematic order of each constituent nematogen, but it predicts excessive anisotropy. Similar to the smooth NI transition in the neat state, the swollen LCEs exhibit continuous changes in volume and shape at the transition temperature without the expected first-order discontinuity. In contrast, swollen polydomain LCEs without a global director exhibit a discontinuous jump in volume at the transitions. Swollen monodomain and polydomain LCEs are strikingly different in the transition behavior, whereas they are similar in the T dependence of the overall volume. These issues remain open questions. The theoretical studies suggest the prominent effects of relative nematicity, cross-interaction strength between swellant and LCE, and the external fields on the anisotropic swelling and phase behavior, but the corresponding experimental study has not been reported thus far. The dynamic aspects of swelling (or shrinking) of LCEs also exhibit unusual features such as a noticeable dimensional overshoot (or undershoot) in the initial stage because the swelling (or shrinking) process consists of shape and volume variation modes with significantly different rates. The former governed by a change in order parameter is much faster than the latter controlled by the diffusion of polymer networks The theoretical modeling for the anisotropic swelling kinetics composed of physically different two modes is an interesting issue.

Swollen monodomain LCEs in unconstrained geometry exhibits an anistropic deformation (more than 10% strain) as well as a significant change in birefringence (more than 90% reduction) in fast response (ca. 10 ms) to electric fields. The pronounced electrooptical and mechanical effects suggest that they are promising materials for electrically driven soft actuators. This electric field response also reveals a deformation mode driven by a globally uniform rotation of the director. The deformation primarily occurs in the plane of director rotation, and the compressive strain along the initial director is proportional to $\sin^2 \theta$ (θ: rotation angle of the director). These characteristics are well described by a soft deformation pathway, although the considerable body tilting in the intermediate stage of director rotation, which was theoretically expected, is not observed. The correlation between the nematic strength and θ dependence of strain is also unclear. The director realignment in constrained geometry results in interesting inhomogeneous patterns as a result of the balance of the Frank elasticity of LCs and rubber elasticity of elastomers. New types of nonuniform director alignment and distortions are expected to emerge under different constraint modes and initial director orientations.

Polydomain LCEs should receive more attention as an interesting LC system of quenched disorder whose correlation length (in the micron range) is considerably greater than the size of the source of disorder (network mesh). The polydomain nature results in slow dynamics that can be observed during shape recovery after the removal of the imposed field and stress relaxation during the P−M transition. The dynamics of polydomain LCEs is strongly affected by whether the cross-links are formed in the isotropic or polydomain nematic state. The characteristic time and domain size steeply increase near T_{NI} when $T \rightarrow T_{NI}$. In order to understand these phenomena, we have to elucidate the balance of the Frank elastic force and random disordering forces and how the cross-linking history and temperature influence these forces.

In this perspective, we have restricted ourselves to the investigation of nematic LCEs and have not considered other types of LCEs including smectic and cholesteric LCEs. A coupling of the orientational order with rubber elasticity in smectic and cholesteric LCEs emerges in a different manner from nematic LCEs, and it yields new physical effects.[5] This will also reveal and develop the potential of smart soft materials having a large variety of functions.

Acknowledgment. The author acknowledges financial support from the Murata Science Foundation, a Grant-in-Aid (No. 16750186), and the 21st century COE program "COE for a United Approach to New Materials Science" from the Ministry of Education, Culture, Sports, Science, and Technology, Japan. The author thanks Prof. M. Warner for providing the figure.

References and Notes

(1) de Gennes, P.-G. *C. R. Acad. Sci., Ser. B* **1975**, *281*, 101.
(2) Küpfer, J.; Finkelmann, H. *Macromol. Chem., Rapid Commun.* **1991**, *12*, 717.
(3) Warner, M.; Terentjev, E. M. *Prog. Polym. Sci.* **1996**, *21*, 853.
(4) Brand, H. R.; Finkelmann, H. Physical Properties of Liquid Crystalline Elastomers. In *Handbook of Liquid Crystals*; Demus, D., Goodby, J., Gray, G. W., Spiess, H.-W., Vill, V., Eds.; Wiley VCH: Weinheim, 1998.
(5) Warner, M.; Terentjev, E. M. *Liquid Crystal Elastomers*; Oxford University Press: Oxford, 2003.
(6) Xie, P.; Zhang, R. *J. Mater. Chem.* **2005**, *15*, 2529.
(7) Brand, H. R.; Pleiner, H.; Martinoty, P. *Soft Matter* **2006**, *2*, 182.
(8) Donald, A. M.; Windle, A. H.; Hanna, S. *Liquid Crystalline Polymers*, 2nd ed.; Cambridge University Press: New York, 2006.
(9) Wermter, H.; Finkelmann, H. *e-Polym.* **2001**, *13*, 1.
(10) Tajbakhsh, A. R.; Terentjev, E. M. *Eur. Phys. J. E* **2001**, *6*, 181.
(11) Donnio, B.; Wermter, H.; Finkelmann, H. *Macromolecules* **2000**, *33*, 7724.
(12) Legge, C. H.; Davis, F. J.; Mitchell, G. R. *J. Phys. II* **1991**, *1*, 1253.
(13) Komp, A.; Rühe, J.; Finkelmann, H. *Macromol. Rapid Commun.* **2005**, *26*, 813.
(14) Vasilets, V. N.; Kovalchuk, A. V.; Yuranova, T. I.; Ponomarev, A. N.; Talroze, R. V.; Plate, N. A. *Polym. Adv. Technol.* **2000**, *11*, 330.
(15) Schuring, H.; Stannarius, R.; Tolksdorf, C.; Zentel, R. *Macromolecules* **2001**, *34*, 3962.
(16) Thomsen, D. L.; Keller, P.; Nacri, J.; Pink, R.; Jeon, H.; Shenoy, D.; Ratna, B. R. *Macromolecules* **2001**, *34*, 5868.
(17) Urayama, K.; Arai, Y. O.; Takigawa, T. *Macromolecules* **2005**, *38*, 3469.

(18) Kempe, M. D.; Scruggs, N. R.; Verduzco, R.; Lal, J.; Kornfield, J. A. *Nat. Mater.* **2004**, *3*, 177.
(19) Ahir, S. V.; Tajbakhsh, A. R.; Terentjev, E. M. *Adv. Funct. Mater.* **2006**, *16*, 556.
(20) Zentel, R. *Liq. Cryst.* **1986**, *1*, 589.
(21) Barnes, N. R.; Davis, F. J.; Mitchell, G. R. *Mol. Cryst. Liq. Cryst.* **1989**, *168*, 13.
(22) Kishi, R.; Kitano, T.; Ichijo, H. *Mol. Cryst. Liq. Cryst.* **1996**, *280*, 109.
(23) Yusuf, Y.; Ono, Y.; Sumisaki, Y.; Cladis, P. E.; Brand, H. R.; Finkelmann, H.; Kai, S. *Phys. Rev. E* **2004**, *69*, 021710.
(24) Urayama, K.; Arai, Y. O.; Takigawa, T. *Macromolecules* **2005**, *38*, 5721.
(25) Tanaka, T. *Sci. Am.* **1981**, *244*, 124.
(26) *Responsive Gels: Volume Transition I*; Dusek, K., Ed.; Adv. Polym. Sci. 109: Springer-Verlag: Berlin, 1993.
(27) Warner, M.; Wang, X. J. *Macromolecules* **1992**, *25*, 445.
(28) Wang, X. J.; Warner, M. *Macromol. Theory Simul.* **1997**, *6*, 37.
(29) Matsuyama, A.; Kato, T. *J. Chem. Phys.* **2001**, *114*, 3817; *J. Chem. Phys.* **2002**, *116*, 8175.
(30) The reported values of S_m for a similar side-chain acrylate-based LCE in the dry state is as large as 0.3.[16]
(31) Brand, H. R.; Kawasaki, K. *Macromol. Rapid Commun.* **1994**, *15*, 251.
(32) Pereira, G. G.; Warner, M. *Eur. Phys. J. E* **2001**, *5*, 295.
(33) Lebar, A.; Kutnjak, Z.; Zumer, S.; Finkelmann, H.; Sánchez-Ferrer, A.; Zalar, B. *Phys. Rev. Lett.* **2005**, *94*, 197801.
(34) Fried, E.; Sellers, S. *J. Chem. Phys.* **2005**, *123*, 044901.
(35) Selinger, J. V.; Jeon, H. G.; Ratna, B. R. *Phys. Rev. Lett.* **2002**, *89*, 225701.
(36) Selinger, J. V.; Ratna, B. R. *Phys. Rev. E* **2004**, *70*, 041707.
(37) Petridis, L.; Terentjev, E. M. *Phys. Rev. E* **2006**, *74*, 051707.
(38) Urayama, K.; Okuno, Y.; Nakao, T.; Kohjiya, S. *J. Chem. Phys.* **2003**, *118*, 2903.
(39) Urayama, K.; Okuno, Y.; Kohjiya, S. *Macromolecules* **2003**, *36*, 6229.
(40) Benmouna, F.; Maschke, U.; Coqueret, X.; Benmouna, M. *Polym. Int.* **2001**, *50*, 469.
(41) Hwang, J. C.; Kikuchi, H.; Kajiyama, T. *Polymer* **1992**, *33*, 1822.
(42) Chi, H.-W.; Kyu, T. *J. Chem. Phys.* **1995**, *103*, 7471. Chi, H.-W.; Zhou, Z. L.; Kyu, T.; Cada, L.; Chien, L.-C. *Macromolecules* **1996**, *29*, 1051.
(43) Urayama, K.; Mashita, R.; Arai, Y. O.; Takigawa, T. *Macromolecules* **2006**, *39*, 8511.
(44) In the case of non-nematogenic polymer networks[45−47] and polydomain LCEs,[23,48] no significant anisotropy is observed in the swelling kinetics even for long cylindrical and thin disk-shaped gels with large anisotropy in the original shape.
(45) Tanaka, T.; Fillmore, D. J. *J. Chem. Phys.* **1979**, *70*, 1214.
(46) Wang, C.; Li, Y.; Hu, Z. *Macromolecules* **1997**, *30*, 4727.
(47) Yamaue, T.; Doi, M. *Phys. Rev. E* **2004**, *69*, 041402.
(48) Urayama, K.; Arai, O. Y.; Takigawa, T. *Macromolecules* **2004**, *37*, 6161.
(49) Mitchell, G. R.; Davis, F. J.; Guo, W. *Phys. Rev. Lett.* **1993**, *71*, 2947.
(50) Roberts, P. M.; Mitchell, G. R.; Davis, F. J. *J. Phys. II* **1997**, *7*, 1337.
(51) Kundler, I.; Fikelmann, H. *Macromol. Rapid Commun.* **1995**, *16*, 679.
(52) Zubarev, E. R.; Kuptsov, S. A.; Yuranova, T. I.; Talroze, R. V.; Finkelmann, H. *Liq. Cryst.* **1999**, *26*, 1531.
(53) Tammer, M.; Li, J.; Komp, A.; Fikelmann, H.; Kremer, F. *Macromol. Chem. Phys.* **2005**, *206*, 709.
(54) Li, J.; Tammer, M.; Kremer, F.; Komp, A.; Finkelmann, H. *Eur. Phys. J. E* **2005**, *17*, 423.
(55) Verwey, G. C.; Warner, M.; Terentjev, E. M. *J. Phys. II* **1996**, *6*, 1273.
(56) Conti, S.; Desimone, A.; Dolzmann, G. *J. Mech. Phys. Solids* **2002**, *50*, 1431.
(57) Fried, E.; Sellers, S. *J. Appl. Phys.* **2006**, *100*, 43521.
(58) Olmsted, P. D. *J. Phys. II* **1994**, *4*, 2215.
(59) Verwey, G. C.; Warner, M. *Macromolecules* **1995**, *28*, 4303.
(60) Urayama, K.; Kondo, H.; Arai, Y. O.; Takigawa, T. *Phys. Rev. E* **2005**, *71*, 051713.
(61) Terentjev, E. M.; Warner, M.; Bladon, H. *J. Phys. II* **1994**, *4*, 667.
(62) A smectic C* LCE shows a finite electrostriction in the neat state because of pronounced ferroelectric effects. See for example: Lehmann, W.; Skupin, H.; Tolksdorf, C.; Gebhard, E.; Zentel, R.; Krüger, P.; Lösche, M.; Kremer, F. *Nature (London)* **2001**, *410*, 447.
(63) Huang, C.; Zhang, Q.; Jákli, A. *Adv. Funct. Mater.* **2003**, *13*, 525.
(64) (a) Urayama, K.; Honda, S.; Takigawa, T. *Macromolecules* **2005**, *38*, 3574. (b) *Macromolecules* **2006**, *39*, 1943.
(65) Yusuf, Y.; Huh, J.-H.; Cladis, P. E.; Brand, H. R.; Finkelmann, H.; Kai, S. *Phys. Rev. E* **2005**, *71*, 061702.
(66) Golubovic, L.; Lubensky, T. C. *Phys. Rev. Lett.* **1989**, *63*, 1082.
(67) Warner, M.; Bladon, P.; Terentjev, E. M. *J. Phys. II* **1994**, *4*, 91.
(68) Hikmet, R. A. M.; Boots, H. M. J. *Phys. Rev. E* **1997**, *51*, 5824.
(69) Chang, C.-C.; Chien, L.-C.; Meyer, R. B. *Phys. Rev. E* **1997**, *56*, 595.
(70) Terentjev, E. M.; Warner, M.; Meyer, R. B.; Yamamoto, J. *Phys. Rev. E* **1999**, *60*, 1872.
(71) Skacej, G.; Zannoni, C. *Eur. Phys. J. E* **2006**, *20*, 289.
(72) Müller, O.; Brand, H. R. *Eur. Phys. J. E* **2005**, *17*, 53.
(73) Verduzco, R.; Meng, G.; Kornfield, J. A.; Meyer, R. B. *Phys. Rev. Lett.* **2006**, *96*, 147802.
(74) Schatzle, J.; Kaufhold, W.; Finkelmann, H. *Makromol. Chem.* **1989**, *190*, 3269.
(75) Clarke, S. M.; Terentjev, E. M.; Kudler, I.; Finkelmann, H. *Macromolecules* **1998**, *31*, 4862.
(76) *Liquid Crystals in Complex Geometries Formed by Polymer and Porous Networks*; Crawford, G. P., Zumer, S., Eds.; Taylor and Francis: London, 1996.
(77) Caggioni, M.; Roshi, A.; Barjami, S.; Mantegazza, F.; Iannacchione, G. S.; Bellini, T. *Phys. Rev. Lett.* **2004**, *93*, 127801.
(78) Buscaglia, M.; Bellini, T.; Chiccoli, C.; Mantegazza, F.; Pasini, P.; Rotunno, M.; Zannoni, C. *Phys. Rev. E* **2006**, *74*, 011706.
(79) Fridrikh, S. V.; Terentjev, E. M. *Phys. Rev. Lett.* **1997**, *79*, 4661; *Phys. Rev. E* **1999**, *60*, 1847.
(80) Küpfer, J.; Finkelmann, H. *Macromol. Chem. Phys.* **1994**, *195*, 1353.
(81) Bergmann, G. H. F.; Finkelmann, H.; Percec, V.; Zhao, M. *Macromol. Rapid Commun.* **1997**, *18*, 353.
(82) Zubarev, E. R.; Talroze, R. V.; Yuranova, T. I.; Plate, N. A.; Finkelmann, H. *Macromolecules* **1998**, *31*, 3566.
(83) Urayama, K.; Okuno, Y.; Kawamura, T.; Kohjiya, S. *Macromolecules* **2002**, *35*, 4567.
(84) Uchida, N. (Dept. Phys., Tohoku Univ., Japan), personal communication.
(85) Elias, F.; Clarke, S. M.; Peck, R.; Terentjev, E. M. *Europhys. Lett.* **1999**, *47*, 442.
(86) ten Bosh, A.; Varichon, L. *Macromol. Theory Simul.* **1994**, *3*, 533.
(87) Uchida, N. *Phys. Rev. E* **2000**, *62*, 5119.
(88) Disch, S.; Schmidt, C.; Finkelmann, H. *Macromol. Rapid Commun.* **1994**, *15*, 303.
(89) Urayama, K.; Honda, S.; Takigawa, T. *Phys. Rev. E* **2006**, *74*, 041709.
(90) Clarke, S. M.; Terentjev, E. M. *Phys. Rev. Lett.* **1998**, *81*, 4436.

MA0623688